Journal of Organometallic Chemistry, 329 (1987) 115–132
Elsevier Sequoia S.A., Lausanne – Printed in The Netherlands

Synthesis, characterization and acid-induced decomposition of 2-aryl-2-ketoethylcobaloximes

Yu-Yuan P. Wo and Kenneth L. Brown*

Department of Chemistry, The University of Texas at Arlington, Arlington, TX 76019 (U.S.A.)

(Received January 16th, 1987)

Abstract

Four substituted 2-phenyl-2-ketoethyl(pyridine)cobaloximes (Ia to Id) have been prepared and characterized. Anaerobic pyrolysis provides the substituted acetophenone (p-$XC_6H_4COCH_3$) as the only product. Complex I rapidly undergoes axial ligand substitution and produces the corresponding aquo complex II in sulfuric acid/water mixtures, and the aquo complex has been verified to undergo acid-induced carbon–cobalt bond cleavage to give substituted acetophenone. A complete rate law which accounts for all of the ionizations of starting materials has been derived and fit to the rate data for decomposition of two of the aquo complexes. The temperature dependence of the decomposition of the fully protonated forms (trications) in strong acid shows that the transition state is "late", characterized by fairly large enthalpies of activation and positive entropies of activation (except for $X = H$) both of which increase with increasing electron withdrawal of X. Experiments in which the p-NO_2 complex was decomposed in D_2SO_4/D_2O confirm that the acetophenone product is initially formed as its enol.

Introduction

Alkylcobalt complexes with protonatable functionalities on the β-carbon of the alkyl ligand (such as OH [1–5] and OR [3,4]) are well known to decompose in aqueous acid to produce olefins. Recently, one of us and others [5] found that 2-aryl-2-hydroxyethylcobaloximes can undergo spontaneous, solvent assisted decomposition to substituted styrenes and acetophenones (Scheme 1, $X = H, CH_3$).

Because of our continued interest in the mechanisms of organocobalt decomposition reactions [1,3–11] it was of interest to extend these observations to alkylcobalt complexes with β-keto functionalities. We have consequently undertaken the synthesis and characterization of a series of p-substituted-2-phenyl-ketoethylcobaloximes (I, II). These interesting compounds, which decompose cleanly in acid to give substituted acetophenones, turn out to be far more stable than their two electron reduced counterparts, the 2-aryl-2-hydroxyethylcobaloximes.

0022-328X/87/$03.50

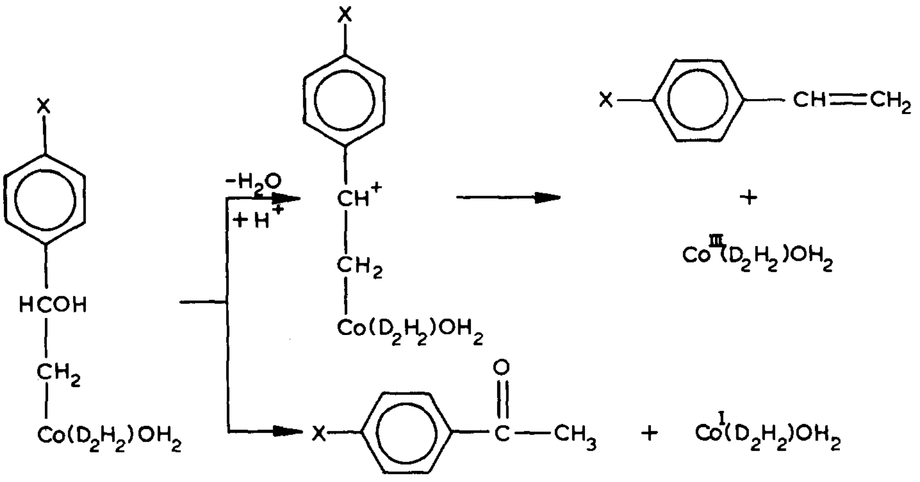

Scheme 1

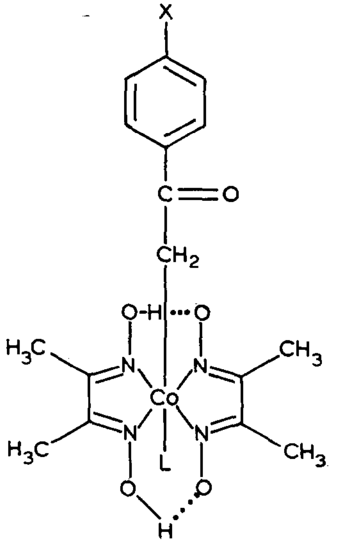

(I : L = py, II : L = OH_2 ;
a : X = H ; b : X = Br ;
c : X = CN ; d : X = NO_2)

Experimental

p-Nitroacetophenone, *p*-acetylbenzonitrile, *p*-bromoacetophenone, α-*p*-dibromoacetophenone, α-bromoacetophenone, cobaltous acetate, dimethylglyoxime, sulfuric acid, potassium hydroxide, benzene and carbon tetrachloride were obtained in the highest purity commercially available and used without further purification. α-Bromo-*p*-cyanoacetophenone was prepared from *p*-acetylbenzonitrile by the free radical bromination procedure [12]. Zinc wool (Fluka) was freshened immediately before use by stirring in 4*N* HCl for several minutes, washing twice with water, drying between paper towels, washing with acetone and air drying. Diethyl ether (Fisher) was distilled from $LiAlH_4$ (Alfa products) to eliminate water, peroxide and stabilizer.

2-Aryl-2-ketoethyl(pyridine)cobaloximes (I) were synthesized by the procedure developed by Roussi and Widdowson [13,14], by using the appropriate alkylating agents. Benzene was the solvent and the reactions were run for 2 h at a temperature of 48° C. The yield of products was 6.5% for Ia, 2.5% for Ib, 2.7% for Ic and 11.6% for Id. NMR ($CDCl_3$): $\delta(Me_4Si)$ 2.44 (s,1.9H), 2.02 (s, 12.0H), 7.28–8.45 (m, 9.4H) for Ia; $\delta(Me_4Si)$ 2.35 (s, 2.0H), 2.06 (s, 12.0H), 7.39–8.51 (m, 9.0H) for Ib; $\delta(Me_4Si)$ 2.39 (s, 2.2H), 2.09 (s, 12.0H), 7.36–8.53 (m, 9.2H) for Ic; $\delta(Me_4Si)$ 2.43 (s, 2.0H), 2.11 (s, 12.0H), 7.34–8.47 (m, 8.7H) for Id.

p-$O_2NC_6H_4COCH_2Co(D_2H_2)OH_2$ (IId) was prepared by the following procedure. 100 mg of Id was dissolved in 50 ml MeOH. With stirring, 10 ml of 5.0 *M* H_2SO_4 was then added dropwise into the solution. The reaction mixture was stirred for 45 min in the dark. 40 ml of water was then added to the solution and about 40 ml MeOH was removed by rotary evaporation. This procedure was repeated three times. The solution was then cooled to 5° C overnight and filtered to recover 25 mg of IId, yield 28.7%. ^1H NMR (methanol-d_4): $\delta(Me_4Si)$ 2.21 (s, 1.9H), 2.24 (s, 12.0H), 7.75–8.31 (m, 4.0H).

All work with 2-aryl-2-ketoethylcobaloximes was performed in dim light with the aid of flashlights, and solutions were covered with aluminum foil whenever possible.

^1H NMR measurements were made on a Varian T-60, Varian EM-360 or Nicolet NT-200 wide bore NMR spectrometer operating at 60.0 or 200.0 MHz.

Spectrophotometric kinetic measurements were recorded on an Applied Physics Corporation Cary 14 or Varian Cary 219 double beam spectrophotometer with sample compartments thermostatted to 25.0 ± 0.1° C or other appropriate temperatures. The first order rate constants at various acidities for pyridine dissociation were obtained from the slopes of $\ln|A_\infty - A_t|$ vs. time at the wavelength with maximum absorbance decrease in the scanning experiments (from 350 nm to 200 nm) on the Cary 14 spectrophotometer. The reaction rates for complex decomposition were determined from the slopes of plots of $\ln|A_t - A_{(t+\Delta t)}|$ against time [15,16] after the absorbances of ca. 5×10^{-5} *M* solutions were continuously monitored and recorded periodically on a Cary 219 spectrophotometer at appropriate wavelengths obtained from scanning experiments.

Acidities of spectrophotometric samples were determined by titration of duplicate aliquots (100–500 μl) with standard KOH to a phenolphthalein endpoint. All such duplicate titrations agreed to within less than 1%. Values of acidity functions were obtained from the determined sulfuric acid molarities from literature data [17–20], interpolating between literature data points when necessary.

Samples for product analysis by ^1H NMR were prepared as follows: 5 mg of complex Ib or Ic was dissolved in 5.0 ml of 5.21 *M* H_2SO_4 solution (i.e. $H_0 = -2.50$). The solutions were then incubated in a 25° C water bath for 3 days. For analysis, the reaction mixtures were extracted five or six times with 1.0 ml of distilled diethyl ether, the pooled ether extracts were evaporated to dryness, and the residues were taken up in 0.5 ml $CDCl_3$ for NMR measurements.

Mass spectrometric analysis were performed on a Finnigan MAT TSQ 46 GC-MS/MS system equipped with a 12 meter Bpl fused silicon capillary column operating at an ionizing potential of 70 eV. The carrier gas (10 lbs head pressure) was He and the injection temperature was maintained at 270 ° C. The retention time was 4.15 min for *p*-nitroacetophenone.

The samples for GC/MS experiments were prepared by a similar procedure as above in H_2SO_4/H_2O or D_2SO_4/D_2O mixtures, as appropriate, and extracted with either diethyl ether or carbon tetrachloride. The pooled extracts were concentrated prior to analysis.

Anaerobic pyrolysis samples for GC/MS and ^1H NMR analysis for product identification were prepared in 1.0 ml Reactivials (Pierce). The vial threads were wrapped with Teflon tape, and then the vials were loosely capped with Teflon Mininert valves (Pierce). A needle was inserted through the rupper septum in the valves and the vials were purged with argon at room temperature for 1 hour. The valves were then screwed tightly onto the vials, the needles were removed and the valves were closed. After the vials were sealed, the samples were pyrolyzed by heating to about 225 ° C for 10 to 15 min, and then cooled. The products were then taken up with diethyl ether. For NMR experiments, the ether was evaporated by passing argon through the solutions and warming them slightly. $CDCl_3$ was then added as solvent for ^1H NMR analysis.

For mass spectral measurements of the incorporation of deuterons from D_2SO_4/D_2O medium into *p*-nitroacetophenone during decomposition of Id, control experiments were performed to determine the amount of acid-catalyzed exchange of the methyl protons of the substituted acetophenone with solvent deuterons. The acidity at which the experimental and control samples were run (0.507 *M* D_2SO_4) was determined by preliminary ^1H NMR measurements of the rate of exchange of solvent deuterons into *p*-nitroacetophenone at several acidities in D_2SO_4. The experimental conditions (acidity and reaction time) were chosen so as to minimize the extent of exchange of product alone in the control experiments (about 16% exchange was anticipated).

Results and discussion

Synthesis and characterization of the 2-aryl-2-ketoethyl(pyridine)cobaloximes

Despite literature reports to the contrary [13] we have been unable to prepare 2-aryl-2-ketoethyl(pyridine)cobaloximes by the standard reductive alkylation procedure [21,22]. Although the yield of such complexes via the Widdowson procedure was poor, sufficient amounts of pure complexes were obtained for the purposes of these studies. Decreasing the reaction temperature to 25 ° C or prolonging the reaction time to 6 h did not appreciably affect the yields.

The 2-aryl-2-ketoethyl(pyridine)cobaloximes (I) are dark brown solids of intermediate polarity. Like most alkylcobaloximes, they are sensitive to light and heat. Anaerobic pyrolysis leads to Co–C bond cleavage, as expected [23,24] and the appropriate substituted acetophenone (p-$XC_6H_4COCH_3$) is produced as determined by ^1H NMR and/or mass spectral identification of the ether soluble products..

With the exception of the CH_2 group in Ia, the ^1H NMR resonances of the methylene group show the expected dependence of chemical shift on the electronic inductive effect of the X group on the p-$XC_6H_4COCH_2$ moiety ($\sigma_p = 0.78$ for NO_2 to 0.0 for H) [25], the more electron-withdrawing X becomes the further downfield the chemical shift. However, the equatorial methyl resonances of I do show a monotonic trend to shift downfield with increasing electron-withdrawal by X.

The UV spectra of these complexes are characterized by an absorption peak at ca. 235–242 nm and a broad shoulder in the range of 275–310 nm. Again, except for Ia, the progression to more electron-withdrawing X is associated with the shift of the peak to longer wavelength.

Spectral changes in aqueous acid

At low acidity (for instance 0.073 *M* H_2SO_4, $H_0 = 1.0$, Fig. 1) the spectrum of Id shows a time-dependent shift of λ_{max} from 242 to 248 nm and an associated decrease in absorbance at $\lambda > 260$ nm. These spectral changes were complete in one hour and the final spectrum was apparently stable for at least another hour. However, subsequent photolysis of the sample produced more dramatic spectral changes including a shift of λ_{max} to 255 nm (the λ_{max} of diaquocobaloxime [4,5]) and larger decrease in absorbance at $\lambda > 275$ nm. This indicates that the carbon–cobalt bond is still intact at the apparent cessation of spectral changes and that the product formed is the aquo complex IId. At higher acidities (for instance 2.124 *M* H_2SO_4, $H_0 = -1.0$, Fig. 2) the spectral changes associated with pyridine dissociation become much more rapid (these are complete within 10 min in Fig. 2) and these are followed by much slower changes including a shift of λ_{max} to 255 nm and decreases in absorbance at $\lambda > 275$ nm. Subsequent photolysis of the sample had no effect on the spectrum. Similar observations were made on Ia, Ib and Ic. It can thus be concluded that at all acidities the dissociation of pyridine from I is much more rapid than acid-induced carbon–cobalt bond cleavage. Thus, the kinet-

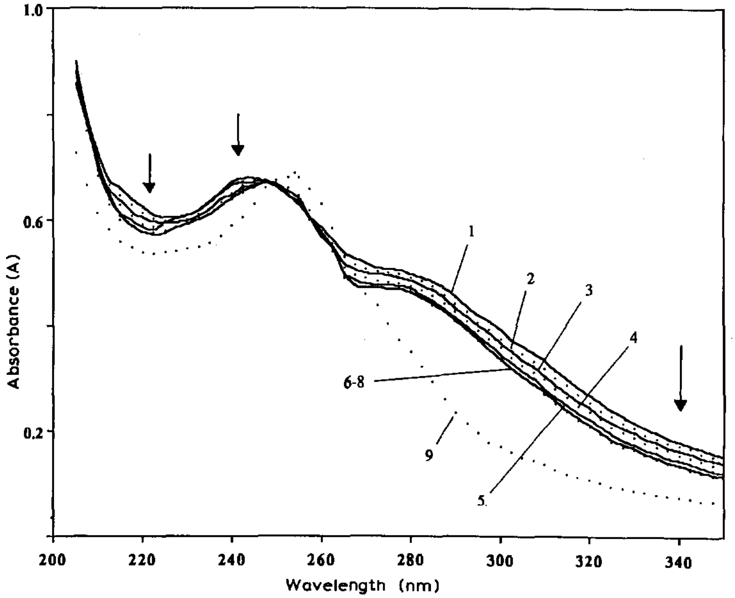

Fig. 1. UV spectra of 3.33×10^{-5} *M* $p\text{-}O_2NC_6H_4COCH_2Co(D_2H_2)py$ (Id) in 0.073 *M* H_2SO_4 ($H_0 = +1.0$) against the reaction time. 1. 0 min, 2. 5 min, 3. 11 min, 4. 22 min, 5. 37 min, 6. 60 min, 7. 114 min, 8. 144 min, 9. 5 min photolysis.

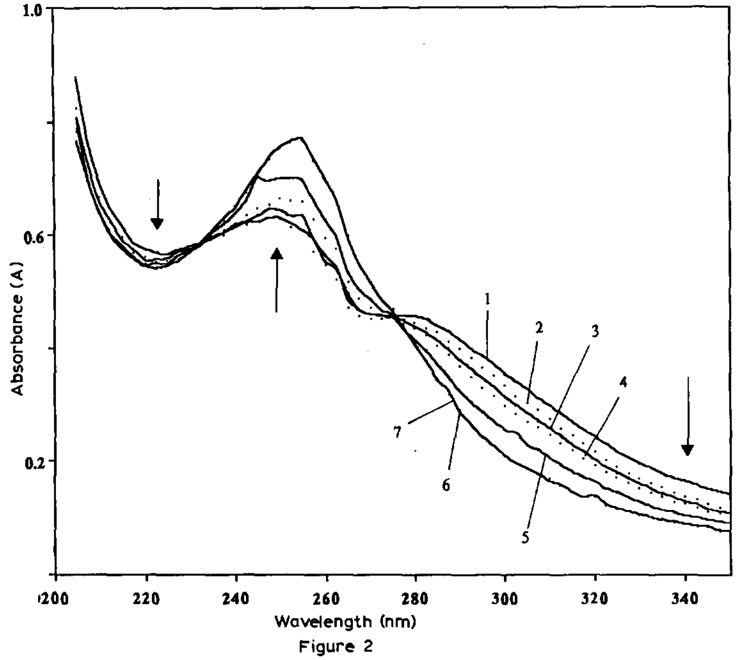

Fig. 2. UV spectra of 3.33×10^{-5} *M* p-$O_2NC_6H_4COCH_2Co(D_2H_2)py$ (Id) in 2.124 *M* H_2SO_4 ($H_0 = -1.0$) against the reaction time. 1. 0 min, 2. 10 min, 3. 100 min, 4. 203 min, 5. 417 min, 6. 1365 min, 7. 1489 min.

ics of the slower process are, in fact, the kinetics of the acid-induced decomposition of II. The increase in the rate of dissociation of pyridine with increasing acidity is in agreement with recent observations [26] that the rate of pyridine dissociation from $CF_3Co(D_2H_2)py$ is greatly increased by the first equatorial protonation of the cobaloxime. The large difference in the rates of pyridine dissociation from I and decomposition of II permit the preparation of the aquo complexes in moderate yield as described in the Experimental section for IId.

Product identification

The products of acid-induced decomposition of I were extracted with diethyl ether from $H_0 = -2.0$ H_2SO_4 solution (after 16 h stirring) and identified by either ^1H NMR (for the products of Ib and Ic) or GC/MS analysis (for the product of Id). *p*-$XC_6H_4COCH_3$ was found to be the only organic product of acid-catalyzed decomposition. For NMR determinations the spectrum of the extracted organic product was shown to be identical to the authentic substituted acetophenone, and both the retention time and mass spectrum of the product of Id decomposition were shown to be identical to those of authentic *p*-nitroacetophenone. Appropriate controls demonstrated that the substituted acetophenones were stable under these reaction conditions.

Kinetics and mechanism of complex decomposition

The decomposition of II was found to be apparently first order at all acidities and gave linear Guggenheim plots (i.e. $\ln|A_t - A_{(t+\Delta t)}|$ vs. time) after the much faster absorbance changes attributed to the pyridine dissociation were complete.

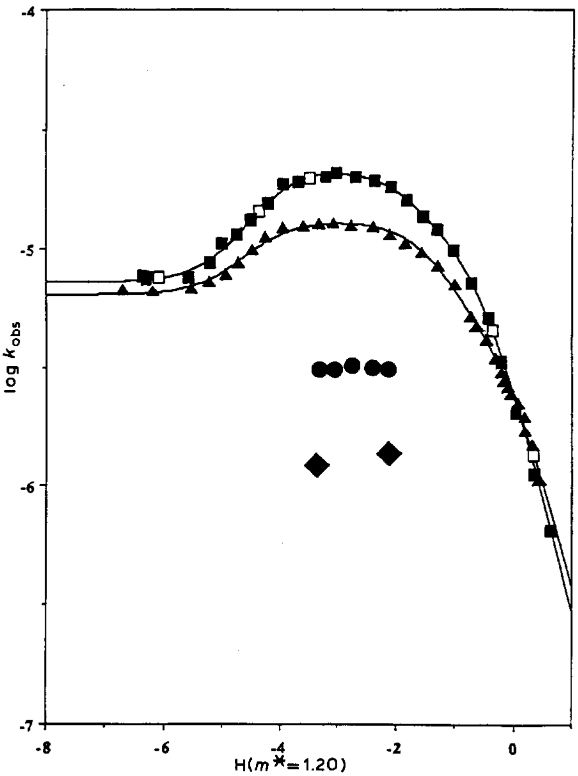

Fig. 3. Plots of log k_{obs} for the decomposition of IIa (◆), IIb (●), IIc (▲), IId (■) and the isolated IId (□) in aqueous sulfuric acid at 25.0 ± 0.1° C vs. H (eq. 1), at $m^* = 1.20$. The solid lines have been calculated from eq. 2 and the kinetic parameters listed in Table 1.

Complete acidity function-rate profiles for IIc and IId and less complete data for IIa and IIb are shown in Fig. 3. Acidity has been expressed via the generalized acidity function (eq. 1) of Cox and Yates [27], where χ is the so-called excess acidity

$$-H = m^*\chi + \log c_{H^+} \tag{1}$$

of sulfuric acid, c_{H^+} is the concentration of hydrogen ion, and m^* is an adjustable parameter characteristic of the type of weak base which is being protonated. The function is based on the observation that all known acidity functions are linearly related to one another [27–29]. In the present work, the m^* value has been set to 1.20 by a method which will be described presently.

In order to confirm that the kinetic data in this H-rate profile of the acid-catalyzed decomposition of I are actually those of the aquo complexes (as inferred from the spectra of Fig. 1 and Fig. 2), the decomposition rate of the isolated complex IId (see experimental section) was measured at five different acidities. The data obtained (open squares) are plotted along with those for Id in Fig. 3. These clearly demonstrated that the measured kinetics refer to the aquo complex, the rate of pyridine dissociation being much faster at all acidities.

The H-rate profiles for the acid-induced decomposition of II are somewhat analogous to those for 2-hydroxyethyl- and 2-alkoxyethyl-cobaloximes [4]. These are

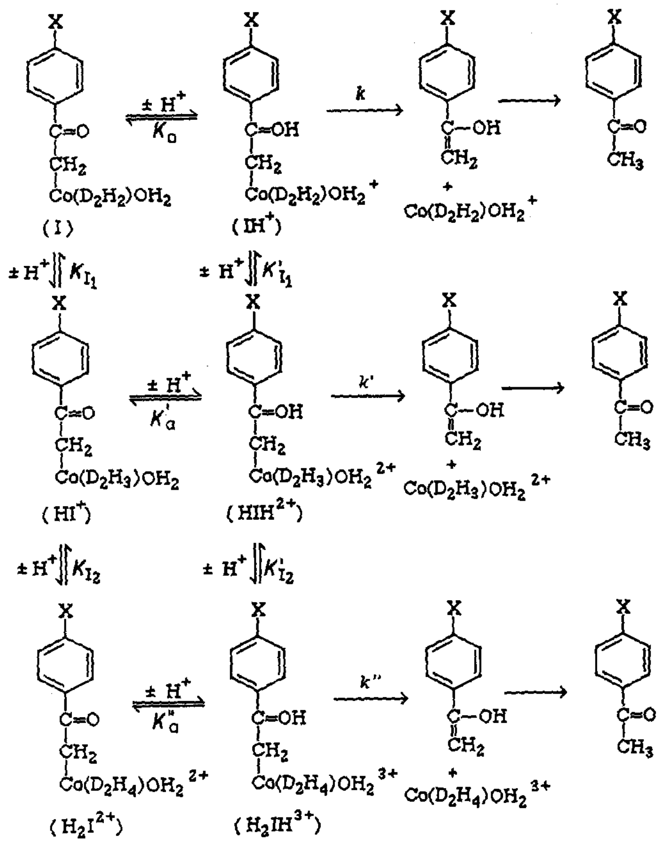

Scheme 2

characterized by a region of first-order dependence on hydrogen ion activity ($H >$ ca. 0.75) followed by an inflection near $H = 0.10$, which is within the reported range of values, 0.67–0.00, for the pK's of the first equatorial protonation of alkyl(aquo)cobaloximes [30,31]. A leveling-off occurs at about $H = -2.0$, which is attributed to the achievement of equilibrium protonation of the carbonyl group. The plateau region is then followed by an acidity-dependent decrease in k_{obs} to an acidity-independent region at $H < -6$. This behavior is apparently due to the second equatorial protonation as previously seen for 2-hydroxyethyl- and 2-alkoxyethyl-cobaloximes. At $H \geq 0.10$, k_{obs} of IIc is slightly larger than that of IId, while the reversed order is observed at all acidities with H values smaller than 0.10.

As cobaloximes are known to undergo two sequential equatorial protonations [4], the complete decomposition scheme including all anticipated ionization of starting materials is shown in Scheme 2. It includes six ionic species and ten microscopic parameters (only eight of which are independent). From the law of mass action and the steady state assumption on the sum of the concentration of intermediates the rate law is thus deduced as in eq. 2, in which, a_{H^+} is the activity of hydrogen ion

$$k_{\mathrm{obs}} = \frac{K'_{\mathrm{I}_1}K'_{\mathrm{I}_2}k a_{\mathrm{H}^+} + K'_{\mathrm{I}_2}k' a^2_{\mathrm{H}^+} + k'' a^3_{\mathrm{H}^+}}{K'_{\mathrm{I}_1}K_{\mathrm{a}}K'_{\mathrm{I}_2} + K'_{\mathrm{I}_2}\left(K'_{\mathrm{a}} + K'_{\mathrm{I}_1}\right)a_{\mathrm{H}^+} + \left(K'_{\mathrm{I}_2} + K''_{\mathrm{a}}\right)a^2_{\mathrm{H}^+} + a^3_{\mathrm{H}^+}} \tag{2}$$

calculated as $a_{H^+} = 10^{-H}$ (eq. 1). According to the ionization scheme (i.e. Scheme 2) for p-$XC_6H_4COCH_2Co(D_2H_2)OH_2$ three macroscopic pK's may be defined as in eqs. 3–8.

$$G_1 = \frac{([HIH^{2+}] + [H_2I^{2+}])a_{H^+}}{[H_2IH^{3+}]} \tag{3}$$

$$G_1 = K'_{I_2} + K''_a \tag{4}$$

$$G_2 = \frac{([IH^+] + [HI^+])a_{H^+}}{[H_2I^{2+}] + [HIH^{2+}]} \tag{5}$$

$$G_2 = \frac{K_{I_2}(K'_a + K'_{I_1})}{K'_a + K_{I_2}} \tag{6}$$

$$G_3 = \frac{[I]a_{H^+}}{[IH^+] + [HI^+]} \tag{7}$$

$$G_3 = \frac{K_{I_1}K_a}{K_a + K_{I_1}} \tag{8}$$

Since $G_1G_2 = K'_{I_2}(K'_{I_1} + K'_a)$ and $G_1G_2G_3 = K'_{I_1}K'_{I_2}K_a$, the rate law can be simplified as in eq. 9.

$$k_{obs} = \frac{K'_{I_1}K'_{I_2}ka_{H^+} + K'_{I_2}k'a^2_{H^+} + k''a^3_{H^+}}{G_1G_2G_3 + G_1G_2a_{H^+} + G_1a^2_{H^+} + a^3_{H^+}} \tag{9}$$

The measured values of k_{obs} at various acidities for Ic and Id were fit to eq. 9 to evaluate the parameters by an iterative, non-linear least-squares method utilizing a simplex minimization algorithm. These data were also used to determine the appropriate $m^\star$ value to be used in conjunction with the generalized acidity function (eq. 1). The approach was to fit the data to eq. 9 using an acidity function based on eq. 1 with an arbitrary value of $m^\star$. This procedure was repeated with different values of $m^\star$. The standard deviation of the fit was found to go through a sharp minimum at $m^\star = 1.20$. The solid lines in Fig. 3 are calculated from eq. 9 using the least-squares parameter values for Ic and Id which are listed in Table 1.

The following points can be noted about the rate law:

(1) k_{obs} was found to be first order in hydrogen ion activity in sufficient dilute acid ($H > 0.5$), and such first order behavior is predicted from the limit of eq. 2 as $a_{H^+} \to 0$, i.e.

$$\lim_{a_{H^+} \to 0} k_{obs} = \frac{k}{K_a} a_{H^+} \tag{10}$$

The limiting slope (k/K_a) values for IId and IIc are 3.01×10^{-6} $M^{-1}s^{-1}$ and 4.07×10^{-6} $M^{-1}s^{-1}$ respectively.

(2) k_{obs} at the plateau region was found to be given by

$$k_{obs}(\text{plateau}) = \frac{K'_{I_2}k'}{K'_{I_2} + K''_a} \tag{11}$$

Table 1

Rate and equilibrium parameters for acid-induced decomposition of p-$XC_6H_4COCH_2Co(D_2H_2)OH_2$ in H_2SO_4/H_2O, 25.0±0.1°C, $m^* = 1.20$ (eq. 1)

Parameters	X = NO_2	X = CN
$K'_{I_1}K'_{I_2}k$	$1.51\times10^{1}\ M^2\ s^{-1}$	$2.95\ M^2\ s^{-1}$
$K'_{I_2}k'$	$4.99\times10^{-1}\ M\ s^{-1}$	$3.99\times10^{-1}\ M\ s^{-1}$
k''	$7.23\times10^{-6}\ s^{-1}$	$6.40\times10^{-6}\ s^{-1}$
$K'_{I_1}K'_{I_2}K_a\ (G_1G_2G_3)$	$5.03\times10^{6}\ M^3$	$7.24\times10^{5}\ M^3$
$K'_{I_2}(K'_a + K'_{I_1})\ (G_1G_2)$	$1.39\times10^{6}\ M^2$	$6.72\times10^{5}\ M^2$
$K'_{I_2} + K''_a\ (G_1)$	$2.27\times10^{4}\ M$	$3.01\times10^{4}\ M$
pG_1	-4.36	-4.48
pG_2	-1.79	-1.35
pG_3	-0.56	-0.03

If $K'_{I_2} \gg K''_a$, k_{obs} is then equal to k'. However, it is not clear if this inequality can be assumed to hold.

(3) At $H < -6$, k_{obs} is observed to be acidity-independent in agreement with the rate equation (eq. 2); since:

$$\lim_{a_{H^+}\to\infty} k_{obs} = k'' \tag{12}$$

The decomposition of IIa and IIb was too slow to be measured at all acidities. In the H-rate profiles (Fig. 3) only a few values of k_{obs} at acidities around the plateau region were determined. These few data, of course, preclude a least squares fit to the rate law. Nevertheless, they allow the estimation of $K'_{I_2}k'/(K'_{I_2} + K''_a)$ (i.e. k_{obs}(plateau), eq. 11) as 1.30×10^{-6} s^{-1} for IIa and 3.16×10^{-6} s^{-1} for IIb. The kinetic parameters which could thus be evaluated for all the complexes are summarized in Table 2.

Figure 4 shows a standard Hammett plot of the data for the acid-induced decomposition of II at the plateau region. The data for this series of complexes yield a good Hammett plot of log k_{obs} vs. σ_p. A least-squares fit of the data provides value of ρ (1.546) and log $k°$ (-5.88). Unfortunately, interpretation of this trend is complicated by the fact that k_{obs}(plateau) does not represent an intrinsic rate constant.

The temperature dependence of the k_{obs} for the decomposition of II in the acid-independent region ($H < -6$) has also been investigated. At these acidities, k_{obs} must represent the rate constant, k'' (eq. 12), for the decomposition of the fully protonated intermediate (H_2IH^{3+} species in Scheme 2). Rate measurements for the decomposition of II in this acidity region (average of several values at H -6.5 to -7.5), over the temperature range 25–75°C are listed in Table 3. As shown in Fig. 5 these data yield good activation plots (i.e. $\ln(k''h/k_bT)$ vs. $1/T$, where h and k_b are Planck's constant and Boltzmann's constant, respectively). The activation parameters ($\Delta H^{\neq}$ and $\Delta S^{\neq}$) are thus determined from the slope and intercept of these plots and are also listed in Table 3. This reaction is characterized by a large positive enthalpy of activation ($\Delta H^{\neq}$). Since $\Delta H^{\neq}$ for IIa and IIb was fairly large, the rate of decomposition of IIa and IIb become fast enough to be measured at higher temperatures. In addition, with the extrapolation of the plot of $\ln(k''h/k_bT)$ vs. $1/T$, k'' at 25°C for IIa and IIb, which was too slow to be measured directly, could be calculated (Table 2).

(Continued on p. 127)

Table 2

The k_{obs}, the calculated ρ value and intercept of Hammett equation for p-$XC_6H_4COCH_2Co(D_2H_2)OH_2$ in H_2SO_4/H_2O at 25.0±0.1° C, $m^* = 1.20$

	Substituents X				ρ	Intercept
	H	Br	CN	NO_2		
σ_p[a]	0	0.23	0.66	0.78		
k/K_a	–	–	$4.07\times10^{-6}\ M^{-1}\ s^{-1}$	$3.01\times10^{-6}\ M^{-1}\ s^{-1}$	−1.100	−4.66
$\frac{K'_{I_2}k'}{K'_{I_2}+K''_a}$	$1.30\times10^{-6}\ s^{-1}$[b]	$3.16\times10^{-6}\ s^{-1}$[b]	$1.33\times10^{-5}\ s^{-1}$	$2.20\times10^{-5}\ s^{-1}$	1.546	−5.88
k''	$1.18\times10^{-6}\ s^{-1}$[c]	$2.61\times10^{-6}\ s^{-1}$[c]	$6.40\times10^{-6}\ s^{-1}$	$7.23\times10^{-6}\ s^{-1}$	0.997	−5.88

[a] Ref. 25. [b] Average of measured k_{obs} at H −2.0 to −3.0. [c] Data from extrapolation of temperature-dependent data, Table 3 and Fig. 5.

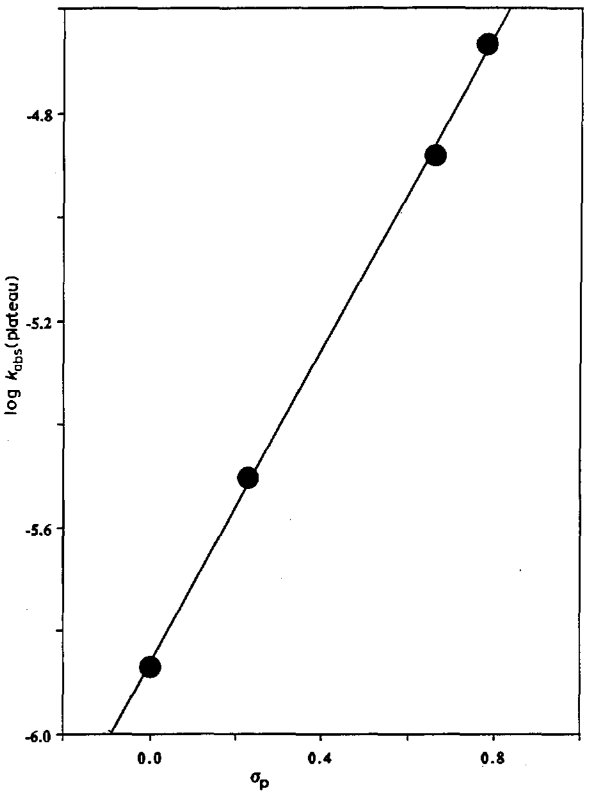

Fig. 4. Hammett plof of log k_{obs}(plateau) (eq. 11) vs. σ_p for the acid-catalyzed decomposition of p-$XC_6H_4COCH_2Co(D_2H_2)OH_2$ ($X = NO_2$, CN, Br and H) at 25.0±0.1°C. The solid line is a least squares fit, slope (ρ) = 1.546, intercept = −5.88.

Table 3

Temperature dependence of the rate constants (i.e. k'') and calculated values of activation enthalpy and activation entropy for p-$XC_6H_4COHCH_2Co(D_2H_4)OH_2^{3+}$

X	Temperature (°C)	k'' (s^{-1})	$\Delta H^{\neq}$ (kcal mol^{-1})	$\Delta S^{\neq}$ (e.u.)
H	45.2	1.83×10^{-5}	25.0±0.3	−1.68±0.91
	54.3	5.94×10^{-5}		
	62.8	1.55×10^{-4}		
	72.5	4.62×10^{-4}		
Br	45.2	4.18×10^{-5}	25.3±1.3	0.76±3.92
	54.3	1.22×10^{-4}		
	62.8	4.14×10^{-4}		
	72.5	1.00×10^{-3}		
CN	25.0	6.40×10^{-6}	27.1±0.7	8.52±2.24
	35.6	2.76×10^{-5}		
	44.7	1.14×10^{-4}		
	53.9	3.88×10^{-4}		
NO_2	25.0	7.23×10^{-6}	27.4±0.6	9.76±2.05
	35.6	3.22×10^{-5}		
	44.7	1.26×10^{-4}		
	53.9	4.71×10^{-4}		

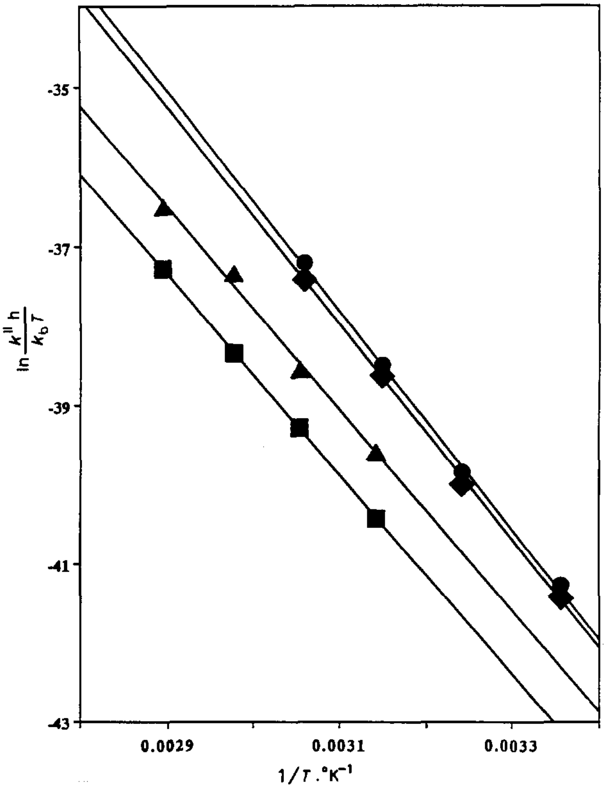

Fig. 5. Plots of $\ln(k''h/k_bT)$ vs. $1/T$ for k'' for decomposition of complex II at $H < -6.5$. The solid lines are least squares fits. IIa, X = H, (■), slope = −12.59, intercept = −0.845; IIb, X = Br, (▲), slope = −12.72, intercept = 0.384; IIc, X = CN, (◆), slope = −13.63, intercept = 4.29; IId, X = NO_2, (●), slope = −13.78, intercept = 4.91.

The data for these complexes generated a satisfactory Hammett plot of log k'' (at 25 °C) vs. σ_p (Fig. 6) with slope (ρ) = 0.997 and intercept (log k'') = −5.878. The variation of the rate constant, k'', is well correlated to the substituent effect.

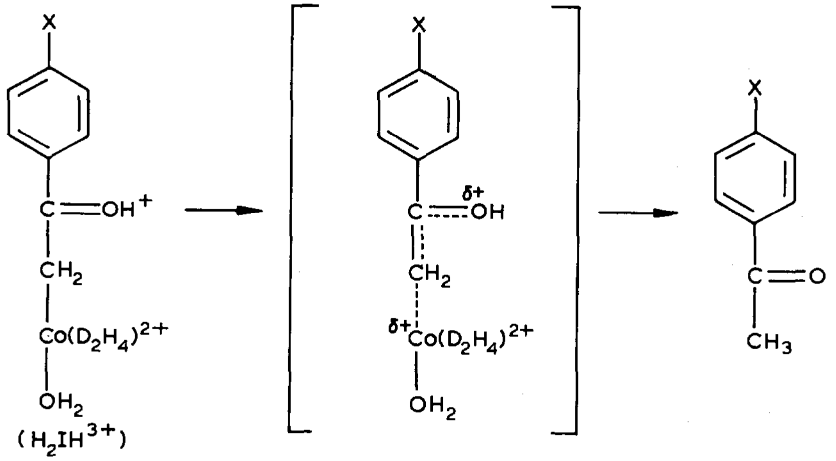

(13)

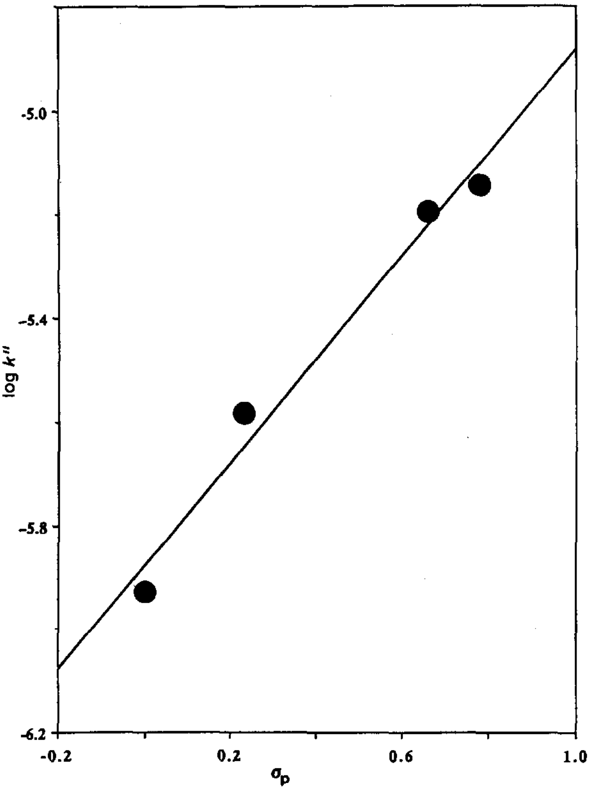

Fig. 6. Plot of log k'' vs. σ_p for p-$XC_6H_4COCH_2Co(D_2H_2)OH_2$ at 25.0 ± 0.1° C. The solid line is a least squares fit, slope (ρ) = 0.997 ± 0.107, intercept (log k''°) = -5.878 ± 0.056.

Electron-withdrawing groups facilitate the cleavage reaction since the bonding electrons of the Co–C bond leave with the organic group as in eq. 13.

In contrast, the limiting values of k_{obs} in dilute acid (i.e. k/K_a, eq. 10, Table 2) show an inverse dependence on σ_p, the value for IId ($\sigma_p = 0.78$) being slightly smaller than that for IIc ($\sigma_p = 0.66$). This can be understood as competition between two opposing effects of the substituent X: electron-withdrawal destabilizes the carbonyl protonated species (IH^+ in Scheme 2) increasing the value of K_a, while electron withdrawal facilitates Co–C bond cleavage (as for k'') increasing k. Apparently, the former effect is slightly larger than the latter one (i.e. the dependence of K_a on X is slightly larger than that of k on X), so that the value of k/K_a decreases with increasing electron withdrawal.

The dependence of $\Delta H^{\neq}$ and $\Delta S^{\neq}$ on the substituent constant σ_p for the decomposition rate of the H_2IH^{3+} species (i.e., k'', Scheme 2) for complex II is shown in Fig. 7 and 8, respectively ($\Delta H^{\neq}$, $\rho = 3.31 \pm 0.34$ and the intercept = 24.82 ± 0.20 kcal mol^{-1}; $\Delta S^{\neq}$, $\rho = 15.4 \pm 1.0$ and the intercept = -2.10 ± 0.55 e.u.). Both $\Delta H^{\neq}$ and $\Delta S^{\neq}$ are correlated to σ_p and both parameters increase significantly with increasing electron withdrawal. Despite the uncertainties regarding the change in solvation of the trication H_2IH^{3+} (eq. 13) as the charge on the carbonyl oxygen is decreased while that on the cobalt center is increased as the transition

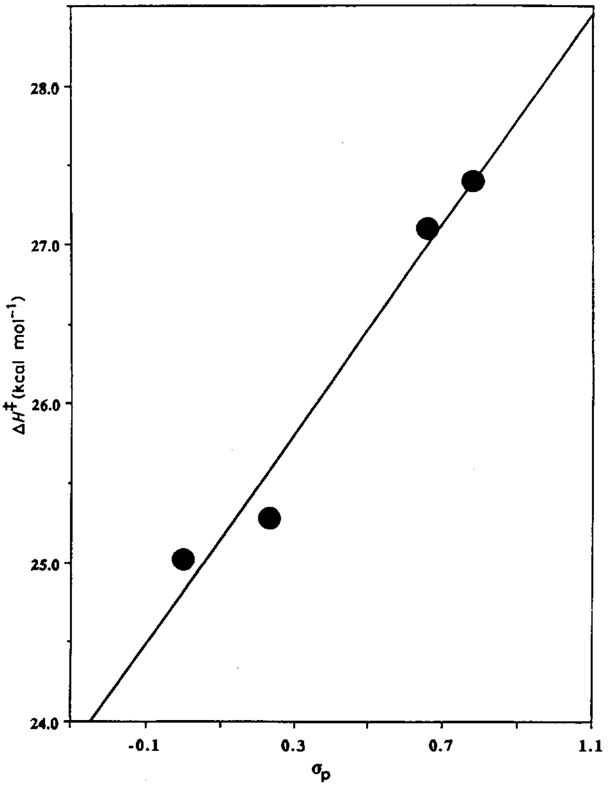

Fig. 7. Plot of $\Delta H^{\neq}$ (enthalpy of activation) vs. σ_p for the decomposition of H_2IH^{3+} (Scheme 2, k''). The solid line is a least squares fit, slope = 3.31 ± 0.34, intercept = 24.82 ± 0.20 kcal mol^{-1}.

state is approached (eq. 13), the large values of $\Delta H^{\neq}$ suggest significant amounts of bond breaking (i.e. Co–C and C=O) in the transition state which are largely uncompensated by bond making (i.e. C=C). The significant increase in $\Delta H^{\neq}$ with σ_p suggests that as the aryl substituent becomes more electron withdrawing, the transition state occurs "later", i.e., the amount of bond breaking in the transition state increases. This conclusion is also demonstrated by the dependence of $\Delta S^{\neq}$ on σ_p which becomes significantly more positive as the substituent becomes more electron withdrawing, clearly indicative of a late transition state. The slightly negative value of $\Delta S^{\neq}$ for IIa (X = H) must presumably indicate the importance of solvent reorganization in the transition state. According to the activation complex theory, the increase in $\Delta H^{\neq}$ should result in a decrease in k''. Since the reverse trend was observed, it is clear that the substituent effect is dominated by the entropic effect.

These results compare favorably to those previously obtained from the temperature dependence of the decomposition of the tricationic species of 2-hydroxyethyl(aquo)cobaloxime (eq. 14) for which $\Delta H^{\neq}$ was 24.7 kcal mol^{-1} and $\Delta S^{\neq}$ was 8.6 e.u. [4]. Although the reaction process of the acid-catalyzed decomposition of II is similar to that of $ROCH_2CH_2Co(D_2H_2)OH_2$ (R = H, CH_3CH_2 or C_6H_5), no evidence for the existence of cobalt(III)-olefinic π-complexes and/or the

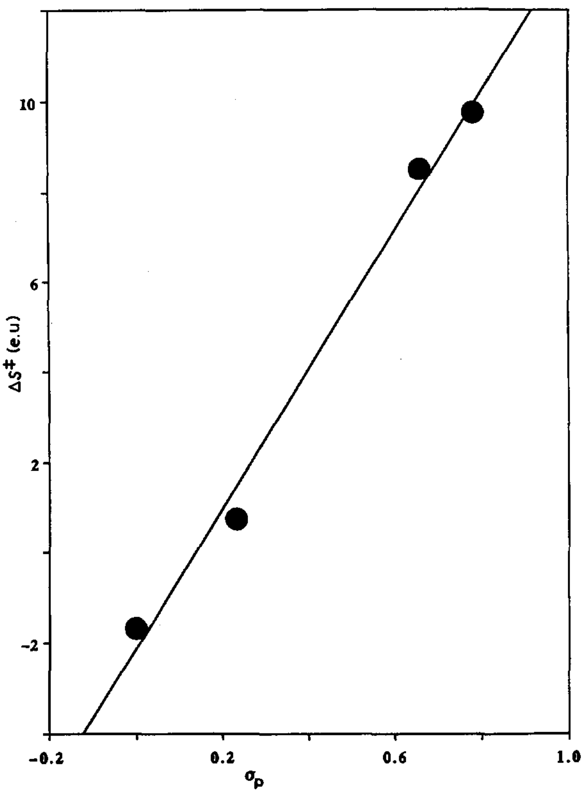

Fig. 8. Plot of $\Delta S^{\neq}$ (entropy of activation) vs. σ_p for the decomposition of H_2IH^{3+} (Scheme 2, k''). The solid line is a least squares fit, slope = 15.4 ± 1.0, intercept = -2.10 ± 0.55 e.u.

electronically equivalent σ-bonded alkylcobalt carbonium ions (which are involved in the reaction of $ROCH_2CH_2Co(D_2H_2)OH_2$) could be found in the present system.

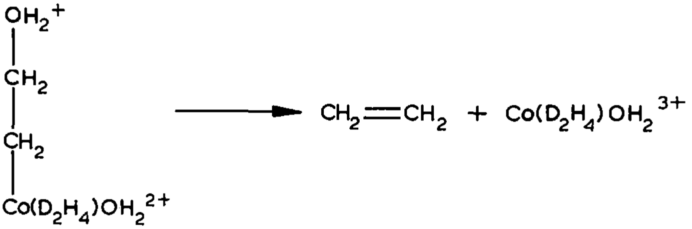

$$OH_2^+-CH_2-CH_2-Co(D_2H_4)OH_2^{2+} \longrightarrow CH_2{=}CH_2 + Co(D_2H_4)OH_2^{3+} \qquad (14)$$

Surprisingly, the structurally analogous complexes p-$XC_6H_4CHOHCH_2Co(D_2H_2)OH_2$ [5] (X = H, CH_3 or CN) were found to decompose many orders of magnitude faster than II, and both substituted styrenes and acetophenones were produced. Furthermore, with low enthalpies of activation ($\Delta H^{\neq} = 2.94 \pm 0.39$ kcal mol^{-1} for $C_6H_5CHOHC\underline{H}_2Co(D_2H_2)OH_2$ and 1.79 ± 0.35 kcal mol^{-1} for p-$CH_3C_6H_4CHOHCH_2Co(D_2H_2)OH_2$), the acetophenone-forming pathway was proposed to be consistent with the base-assisted 1,2-hydride shift process (eq. 15) with an

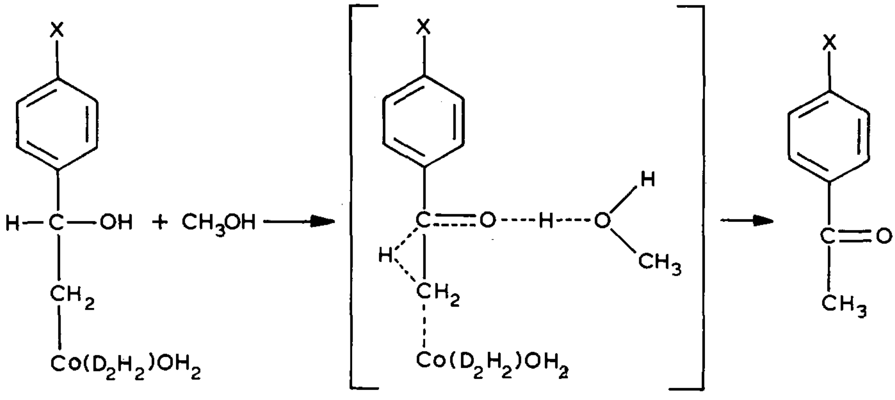

(15)

early transition state. All of these suggest the β-hydrogen should play a significant role in the modification of the mechanism for the decomposition of alkyl(aquo)cobaloximes.

In order to demonstrate, as the proposed mechanism demands, that the immediate product of the acid-catalyzed decomposition reaction is the enol of the substituted acetophenone, the percentage of deuterium incorporation into the methyl group of p-$O_2NC_6H_4COCH_3$ during the decomposition of Id in D_2SO_4/D_2O was investigated. From ^1H NMR measurements of the exchange of solvent deuterium into p-$O_2NC_6H_4COCH_3$ in 0.56 M D_2SO_4/D_2O at 25 °C ($k_{obs} = 2.75 \times 10^{-6}$ s^{-1}) the percent deuterium exchange was calculated to be about 16% after 16 h stirring at room temperature. Under the same conditions, based on the measured k_{obs} (7.0×10^{-6} s^{-1}) of acid-induced decomposition for IId in this medium, 33% decomposition was anticipated. The isotopic composition of the acetophenone products for both a control sample of p-$O_2NC_6H_4COCH_3$ and a sample of Id in 0.56 M D_2SO_4 were determined by mass spectrometry after extraction with diethyl ether and concentration. 16.5%-d_1, 1.6%-d_2 and 0.1%-d_3 p-$O_2NC_6H_4COCH_3$ were obtained for the control sample. This is consistent with the calculated value of isotopic exchange (16%) from ^1H NMR measurements. However, the p-nitroacetophenone product recovered from the decomposition of Id was found to be only 42.2%-d_1, 2.6%-d_2 and 0.5%-d_3. This is apparently due to the unexpected solubility of the unreacted pyridine (Id) and/or aquo (IId) complexes in the extracting solvent (diethyl ether) and its subsequent pyrolysis in the GC injector (270 °C) leading to undeuterated p-nitroacetophenone. Measurement of the solubility of Id and IId in diethyl ether allowed correction of the extent of monodeuteration of the reaction product to 73%. In order to confirm this result, the experiment was repeated using CCl_4 as the extracting solvent in which Id and IId proved to be somewhat less soluble. The control for p-nitroacetophenone showed 19.4%-d_1, 2.1%-d_2 and 0.2%-d_3. The experimental sample now showed 56.8% monodeuteration which was increased to over 80% by correction for the solubility of Id and IId in CCl_4. In addition, the hypothesis of pyrolysis of unreacted starting material in the GC injector was tested by rerunning the experimental sample at an injector temperature of 200 °C (the lowest temperature at which sufficient rapid vaporization of p-nitroacetophenone could be achieved). This increased the observed monodeuteration of the product (without correction for solubility) to 58.6%. These results provide good evidence that the acetophenone product is initially formed as the enol, thus providing further substantiation of the mechanism of Scheme 2.

Acknowledgements

This research was supported by the Robert A. Welch Foundation, Houston, Texas, Grand No. Y-749 (K.L.B.). The authors would also like to thank Dr. D.S. Marynick for his help with the non-linear least-squares treatment and Alcon Laboratories, Fort Worth, Texas, for providing access to the Finnigan MAT TSQ 46 GC/MS/MS system and especially to Dr. Jim Hudson for his help with the experiments on this instrument.

References

1 K.L. Brown, and L.L. Ingraham, J. Am. Chem. Soc., 96 (1974) 7681.
2 J.H. Espenson, and D.M. Wang, Inorg. Chem., 18 (1979) 2853.
3 K.L. Brown, and S. Ramamurthy, Organometallics, 1 (1982) 413.
4 K.L. Brown, S. Ramamurthy, and D.S. Marynick, J. Organomet. Chem., 287 (1985) 377.
5 K.L. Brown, O. Perkins, Z. Szeverenyi, and A. Fulep-Poszmik, J. Organomet. Chem., 302 (1986) 101.
6 K.L. Brown, M.M.L. Chu, and L.L. Ingraham, Biochemistry, 15 (1976) 1402.
7 K.L. Brown, Inorg. Chim. Acta, 31 (1978) L401.
8 K.L. Brown, J. Am. Chem. Soc., 101 (1979) 6600.
9 K.L. Brown, and R.K. Hessley, Inorg. Chem., 19 (1980) 2410.
10 K.L. Brown, and R.K. Hessley, Inorg. Chim. Acta, 53 (1981) L115.
11 K.L. Brown, J. Chem. Soc., Chem. Commun., (1981) 589.
12 H.O. House, Modern Synthetic Reactions, 2nd edit., W.A Benjamin Inc., Menlo Park, 1971, p. 459–460.
13 P.F. Roussi, and D.A. Widdowson, J. Chem. Soc., Chem. Commun., (1979) 810.
14 P.F. Roussi, and D.A. Widdowson, J. Chem. Soc., Perkins Trans. I, (1982) 1025.
15 E.A. Guggenheim, Philos. Mag., 2 (1926) 538.
16 J.W. Moore, and R.G. Pearson, Kinetics and Mechanisms, 3rd ed., McGraw-Hill Wiley&Sons, New York, 1981, p. 70–72.
17 C.H. Rochester, in A.T. Blomquist (Ed.), Activity Functions, Academic Press, New York, 1970, p. 24.
18 L.P. Hammett, and A.J. Deyrup, J. Am. Chem. Soc., 54 (1932) 2721.
19 K.N. Bascombe, and R.P. Bell, J. Chem. Soc., (1959) 1096.
20 R.S. Ryabova, I.M. Medvetskaya, and M.T. Vinnik, Zh. Fiz. Khim., 40 (1966) 339.
21 G.N. Schrauzer, Inorg. Synth., 11 (1968) 61.
22 A.L. Crumbliss, and P.L. Gaus, Inorg. Chem., 14 (1975) 486.
23 G.N. Schrauzer, J.W. Sibert, and R.J. Windgassen, J. Am. Chem. Soc., 90 (1968) 6681.
24 G.N. Schrauzer, Acc. Chem. Res., 1 (1968) 97.
25 C.D. Johnson, The Hammett Equation; Cambridge University Press, 1973.
26 K.L. Brown, and T.-F. Yang, Inorg. Chem., in press.
27 R.A. Cox, and K. Yates, J. Am. Chem. Soc., 100 (1978) 3861.
28 N.C. Morziano, G.M. Cimino, and R.C. Passerini, J. Chem. Soc., Perkin Trans. II, (1973) 1915.
29 J.F. Bunnett, and F.P. Olsen, Can. J. Chem., 44 (1964) 1899.
30 J.H. Espenson, and T.H. Chao, Inorg. Chem., 16 (1977) 2553.
31 A. Adin, and J.H. Espenson, Chem. Commun., (1971) 653.